Bioorganic & Medicinal Chemistry 19 (2011) 3855–3863

Contents lists available at ScienceDirect

Bioorganic & Medicinal Chemistry

journal homepage: www.elsevier.com/locate/bmc

Biological activity of water-soluble inclusion complexes of 1′-acetoxychavicol acetate with cyclodextrins

Hideki Azuma [a,*], Yui Aizawa [a], Nao Higashitani [a], Takashi Tsumori [a], Akiko Kojima-Yuasa [b], Isao Matsui-Yuasa [b], Takeshi Nagasaki [a]

[a] Department of Applied Chemistry and Bioengineering, Graduate School of Engineering, Osaka City University, Sugimoto 3-3-138, Sumiyoshi-ku, Osaka 558-8585, Japan
[b] Department of Food and Human Health Sciences, Graduate School of Human Life Sciences, Osaka City University, Sugimoto 3-3-138, Sumiyoshi-ku, Osaka 558-8585, Japan

ARTICLE INFO

Article history:
Received 5 April 2011
Revised 19 April 2011
Accepted 20 April 2011
Available online 22 April 2011

Keywords:
1′-Acetoxychavicol acetate
Water-soluble complex
Cyclodextrin
High-speed vibration milling
Apoptosis
Antitumor

ABSTRACT

1′-Acetoxychavicol acetate (ACA), isolated from the rhizomes and the seeds of the *Zingiberaceae* plant, has a variety of biological activities such as antitumor, antiallergic and repellent effects. However, ACA seems to have some disadvantages which may limit for future possible clinical applications, for example, its poor water solubility. Furthermore, ACA is not stable in aqueous solutions and undergoes hydrolysis and/or isomerization. To improve the solubility and stability of ACA in water, we prepared the inclusion complexes with various β-cyclodextrins (β-CDs).In aqueous solution, the association constants of ACA with various CDs were estimated at 662 ± 95 (β-CD), 336 ± 70 (methyl-β-CD, Meβ-CD), and 322 ± 44 M^{-1} (hydroxypropyl-β-CD, HPβ-CD), respectively, by a spectrofluorometric displacement method based on competition between a guest and a fluorescent probe for CDs. It was revealed that almost all ACAs existed as a free molecule in the CD-containing aqueous solution. However, in the case of preparing the inclusion complexes of CDs with ACA by a solid phase 'high-speed vibration milling' technique, the average inclusion rates of the obtained water-soluble complexes were calculated as 88 ± 13% (β-CD), 70 ± 1% (Meβ-CD), and 63 ± 2% (HPβ-CD), respectively, by ^{1}H NMR analysis. To characterize the structures of the CD·ACA complexes, 2,3,6-trimethyl-β-CD (TMeβ-CD)·ACA complex was prepared as a model compound (inclusion rate: 40%). As a result of 2D ROESY experiments, it was considered that the aromatic ring of ACA is located in the narrow side of the hydrophobic cavity of the TMeβ-CD and both 1′- and 4-acetoxy groups of ACA positioned in the vicinity of the secondary and primary methoxy groups of TMeβ-CD, respectively. Furthermore, we examined the apoptogenic activity of CD·ACA complexes to evaluate whether or not the bioactivities of ACA were affected by their inclusion. Although the cytotoxicity of all CD·ACA complexes in human epithelial carcinoma HeLa cells and murine adenocarcinoma colon26 cells were diminished as compared with the ACA alone, only HPβ-CD·ACA maintained high levels of activity. In addition, HPβ-CD·ACA, and Meβ-CD·ACA showed suppressive effect for the transcription factor NF-κB activation on LPS-activated murine macrophage RAW264.7 cells and the former was more active complex. Furthermore, HPβ-CD·ACA inhibited the in vivo tumor growth of tumor-bearing mice, although the activity was slightly weak compared with that of free ACA. These results indicate that HPβ-CD is the best host molecule for ACA to form a water-soluble complex with the similar biological activity of free ACA.

1. Introduction

1′-Acetoxychavicol acetate (ACA), isolated from the rhizomes and the seeds of the *Zingiberaceae* plant such as *Languas galanga* and *Alpinia galanga*, which is used as a ginger substitute and a stomach medicine in Southeast Asia, has a variety of biological activities including antitumor,[1–4] antiallergic,[5] anti-human immunodeficiency virus (HIV) activity,[6] induction of nitric oxide production,[7,8] and inhibition of interferon-β production.[9] More recently, our group reported that natural-type (*S*)-ACA caused a rapid decrease of intracellular glutathione levels by the depression of glutathione reductase activity in Ehrlich ascites tumor cells.[10]

Thus, ACA has a variety of useful biological properties; however, ACA seems to have some disadvantages which may limit for future possible clinical applications, for example, its poor solubility in water. In fact, polar organic solvents such as DMSO or ethanol should be used to dissolve it in aqueous solution. Furthermore, ACA is not stable in aqueous solutions and undergoes hydrolysis and/or isomerization.[11]

Various solubilizing and stabilizing techniques have been developed for water-insoluble compounds, but the most popular

* Corresponding author. Tel./fax: +81 6 6605 2168.
E-mail address: azumah@bioa.eng.osaka-cu.ac.jp (H. Azuma).

0968-0896/$ - see front matter © 2011 Published by Elsevier Ltd.
doi:10.1016/j.bmc.2011.04.038

procedure remains the inclusion of substances within cyclodextrins (CDs). The α-, β- and γ-CDs are naturally occurring, water-soluble, cyclic oligosaccharides constituted by six, seven, and eight glucopyranoside units, respectively. They have a truncated cone shape containing a hydrophobic inner cavity and hydrophilic outer surfaces. CDs have an ability of including various lipophilic 'guest' molecules into their hydrophobic cavity via noncovalent interactions such as van der Waals forces or hydrophobic interactions in relatively polar solvents. Therefore, CDs are widely used as solubilizers and stabilizers for a variety of poorly soluble and labile drugs by forming inclusion complexes in pharmaceutical formulations.[12,13] However, in general, complexation efficiency of CDs is poorly. Therefore, relatively large amounts of CDs are needed to form the complex with the drugs.

Komatsu et al. reported the method of the preparation of a water-soluble C60·γ-CD complex by a mechanochemical 'high-speed vibration milling' technique (HSVM).[14] Ikeda et al. demonstrated to solubilize the single-wall carbon nanotubes with γ-CD in an aqueous solution by HSVM.[15] Thus, the solid phase HSVM technique is highly effective for poorly water-soluble molecules with aqueous host molecules such as CDs although the mechanism of the complexation remains unclear.

The aim of this work was to investigate the preparation of water-soluble solid complexes of readily preparable racemic ACA with native or modified CDs by HSVM. Furthermore, some biological properties of CD·ACA complexes, namely, apoptosis-inducing activity and inhibition effect on lipopolysaccharide (LPS)-induced NF-κB activation, and antitumor activity on tumor-bearing mice were also studied.

2. Results and discussion

2.1. Complexations of ACA with various cyclodextrin in aqueous solution

The association constants (K) of ACA with various CDs in aqueous solution were estimated by a spectrofluorometric displacement method based on competition between a guest and a fluorescent probe for CDs described by Tee et al.[16] Sodium 1-anilino-8-naphthalenesulfonate (ANS) is barely fluorescent in aqueous solution. However, ANS is very sensitive to environmental changes, therefore, widely used as a competition probe to investigate the inclusion complex of cyclodextrins with a guest molecule. First, spectrofluorimetric titrations were performed in PBS solution (pH 7.4) to determine the association constants (K_{ANS}) of various β-CDs with ANS. In the case of the formation of 1:1 complex between CD and ANS, the relative fluorescence intensity F_{rel} ($=I_{obs}/I_0$) varies with the concentration of CD in accord with Eq. 1.[16,17]

$$F_{rel} = \frac{(1/K_{ANS} + F_c[CD])}{(1/K_{ANS} + [CD])} = \frac{1 + F_c K_{ANS}[CD]}{1 + K_{ANS}[CD]} \quad (1)$$

On the basis of Eq. 1, a typical plot is shown in Figure 1A. Values of K_{ANS} and F_c were estimated from nonlinear fitting of Eq. 1 and listed in Table 1. The fluorescence intensity of ANS in the presence of each CD was decreased dose-dependently by the addition of ACA (Fig. 1B).The K values of various CDs with ACA were estimated from these results (see Section 4) and listed in Table 1. β-CD showed a highest K value (661 M^{-1}) and modifications of CD diminished the association with ACA. This result revealed that almost all ACAs existed as a free molecule in the CD-containing aqueous solution at micro-order concentration. For instance, in the presence of 20 μM β-CD and 20 μM ACA, which is a popular concentration of ACA for the studies, the rate of the existence of β-CD·ACA complex is calculated as about 1%. Unfortunately, we could not estimate the K values for α- and γ-CD because the fluorescence intensities of the complexes of these CDs with ANS were invariant (α-CD), or slightly increased (γ-CD). Probably, α-CD could not form the complex with ACA and γ-CD was available to form the ternary complex with ANS and ACA in aqueous solution.

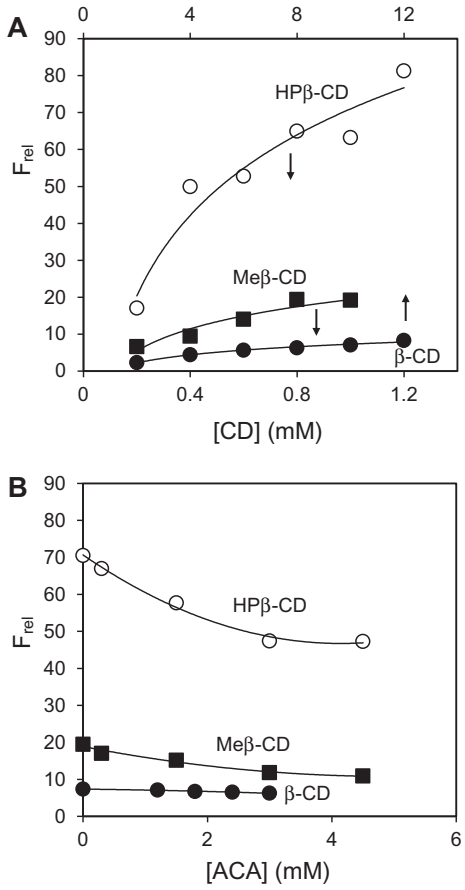

Figure 1. (A) Effects of added CDs on the fluorescence of ANS in 3% ethanol-including PBS solution (pH 7.4); (B) competitive effects of ACA on the fluorescence of ANS in the presence of CDs; $F_{rel} = I_{obs}/I_0$.

Table 1
Association constants of various CD with ANS or ACA

CDs	Literature values[a]		This work[b]		
	F_c	K_{ANS} (M^{-1})	F_c	K_{ANS} (M^{-1})	K (M^{-1})
β-CD	46.7	37.3	16.9	16.9	662 ± 95
Meβ-CD			58.5	58.5	336 ± 70
HPβ-CD	430	585	428	428	293 ± 66

[a] At 25 °C, in 0.2 M phosphate buffer (pH 11.6, Ref. 16).
[b] At 25 °C, in PBS (pH 7.4) with 3% ethanol.

2.2. Complexations of ACA with various cyclodextrins by HSVM

Mixtures of CDs and 5 M equiv of ACA were placed in an agate capsule together with two agate mixing balls. They were vigorously mixed by shaking at a rate of 25 Hz for 60 min by the use of a high-speed vibration mill. The solid mixtures were dissolved in water and centrifuged at 10,000g for 10 min. The resulting supernatants were filtered and lyophilized to obtain the various CD·ACA complexes and almost all amounts of CDs were recovered. As an example, Figure 2A shows the ^{1}H NMR spectrum of the Meβ-CD·ACA complex in D_2O along with the assignments of key resonances for estimating the values of the inclusion rate of ACA into

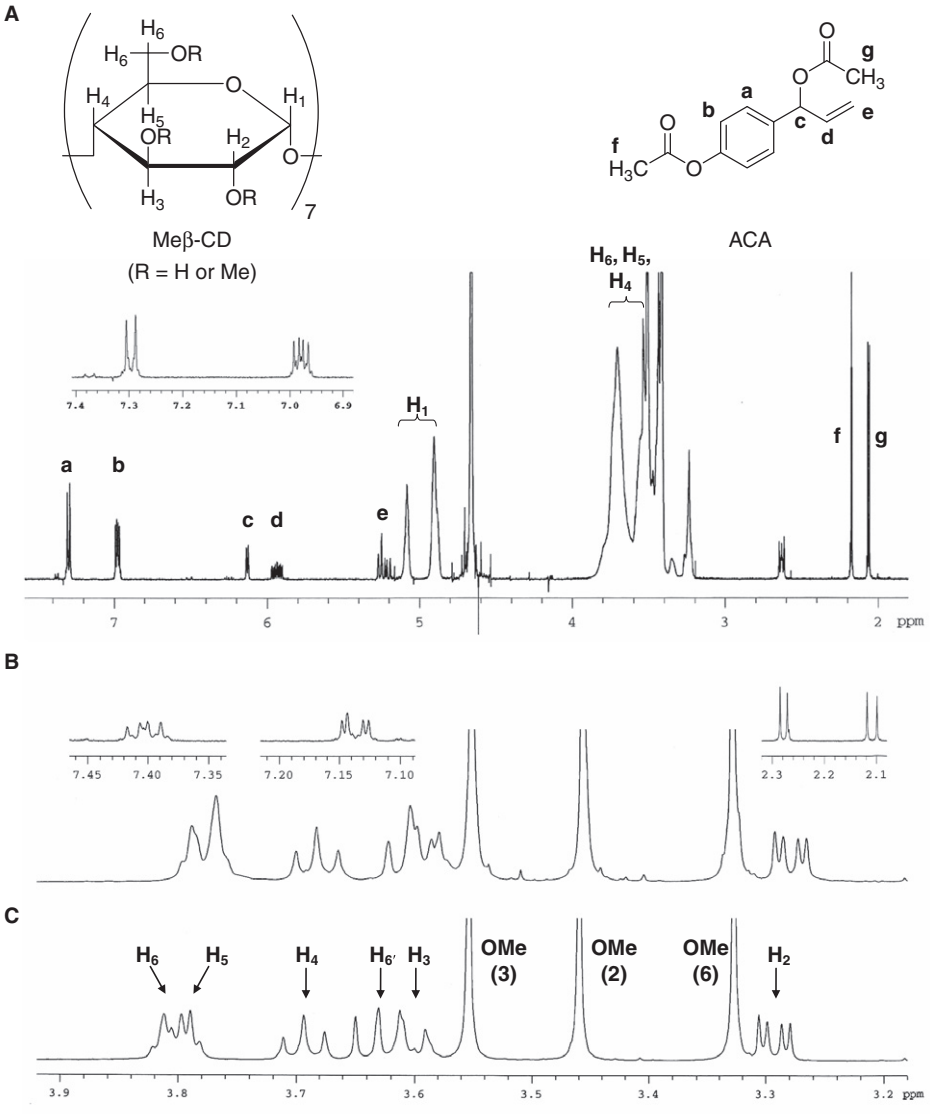

Figure 2. (A) ^{1}H NMR spectrum of the Meβ-CD·ACA complex in D_2O; (B) selected region of the NMR spectrum of TMeβ-CD·ACA with inset showings the peaks corresponding to the aromatic protons and the acetoxy groups of ACA in D_2O; (C) selected region of the NMR spectrum of TMeβ-CD in D_2O.

Meβ-CD. The inclusion rate of ACA was calculated as 69%, by the integrated ratio of seven H1 protons of Meβ-CD to the aromatic proton *a* of ACA. The average values were listed in Table 2 and revealed that β-CD was the best host molecule for ACA and the inclusion rates of ACA in the complexes were relevant to the association constants in aqueous solution (Table 1). In the cases of Meβ-CD and HPβ-CD, the inclusion rates were similar when equimolar amounts of CDs and ACA were mixed.

Table 2
Inclusion rates of ACA in the complexes obtained by HSVM

CDs	Inclusion rate (%)	
	CD/ACA = 1:5	CD/ACA = 1:1
α-CD	44 ± 6	
β-CD	88 ± 13	76 ± 4
γ-CD	65 ± 5	
Meβ-CD	70 ± 1	69 ± 1
HPβ-CD	63 ± 2	66 ± 4

The inclusion rates of ACA in the complexes were determined by ^{1}H NMR analysis of the complex in D_2O.

Two significant splits of the peaks were observed at 2.06 ppm (singlet to doublet splitting) and 6.99 ppm (doublet to double doublet splitting) which are assigned as 1′-acetoxy methyl proton *g* and the aromatic proton *b* on C-3 carbon of ACA, respectively (Fig. 2A). To determine the geometry of the inclusion complex, rotating frame nuclear Overhauser effect spectroscopy (ROESY) of the Meβ-CD·ACA complex was carried out in D_2O.[12,18] Weak intermolecular ROE correlations were observed between the aromatic protons of ACA and the H6′ (or H4 proton, 3.6–3.68 ppm), H5 and H6 (3.76–3.86 ppm) protons of Meβ-CD (data not shown). However, it was difficult to determine which proton lying on the inner surface of Meβ-CD to correlate with the aromatic protons of ACA, because the host compound is a randomly *O*-methylated β-CD. Therefore, unmodified β-CD or 2,3,6-tri-*O*-methyl-β-CD (TMeβ-CD) were used as a host molecule to obtain the detail of the geometry of cyclodextrin and ACA complex prepared by HSVM. Unfortunately, only very weak intermolecular ROE correlations was also observed in the β-CD·ACA complex (data not shown). On the other hand, intermolecular ROE correlation between the aromatic proton *a* of ACA and the H3 (or H6) and H5 (or H6) protons of TMeβ-CD was observed (Fig. 3). Strong correlation between

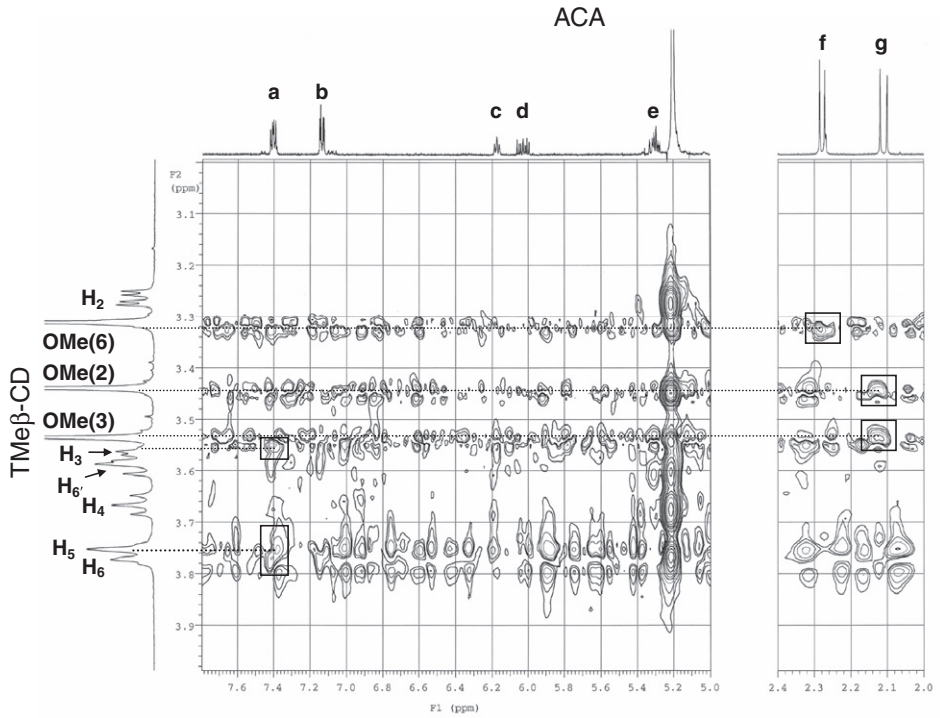

Figure 3. Selected regions of the 2D ROESY spectrum of the TMeβ-CD·ACA complex (inclusion rate: 40%) in D_2O.

the 1′-acetoxy methyl group of ACA and the methoxy groups on C-2 and C-3 carbons of TMeβ-CD indicates that the former is in spatial proximity to the secondary methoxy groups on the wide rim of TMeβ-CD. Furthermore, the correlation between the 4-acetoxy methyl proton *f* of ACA and the primary methoxy groups of TMeβ-CD was also observed. Weak intermolecular ROE correlations were also observed between the aromatic proton *a* of ACA and the H3 and H5 protons of TMeβ-CD. However, the correlation between the proton *b* of ACA and the protons of TMeβ-CD was unclear although both two peaks of ACA phenyl protons were divided into double doublet in ^{1}H NMR (Fig. 2B).

These findings suggested a possible geometry of the complex as follows: (i) the aromatic ring of ACA was located in the narrow side of the hydrophobic cavity of the TMeβ-CD; (ii) the 1′-acetoxy group of ACA positioned in the vicinity of the secondary methoxy groups on C-2 and C-3 carbons of TMeβ-CD; (iii) the 4-acetoxy moiety of ACA lay in the proximity of the methoxy groups on C-6 carbons of TMeβ-CD. A possible structure of the TMeβ-CD·ACA ((*S*)-isomer) complex was showed in Figure 4. Because of the configuration of the TMeβ-CD·ACA complex, it is considered that no intermolecular ROE correlation between two acetoxy groups of ACA and three kinds of hydroxy moieties of β-CD (or Meβ-CD) is observed.

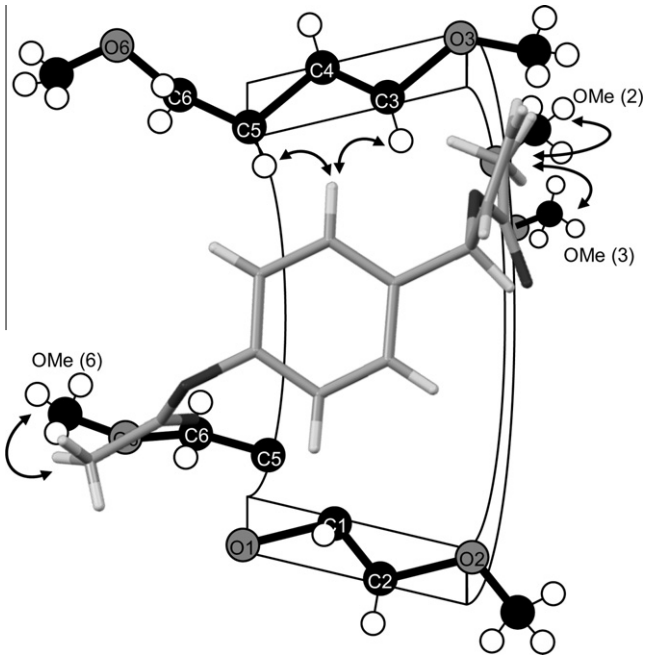

Figure 4. A possible structure of the TMeβ-CD·(*S*)-ACA complex derived from 2D ROESY spectrum. Conformation of (*S*)-ACA was predicted from the X-ray crystal structure analysis of the racemic ACA.

2.3. Stability of the cyclodextrin-included ACA

Yang et al. reported that ACA was not stable in 5% ethanol-containing aqueous solution at 60 °C and 1′-hydroxychavicol acetate, *p*-coumaryl diacetate, and *p*-acetoxycinnamic alcohol were generated from ACA by a hydrolysis or [3,3] sigmatropic rearrangement.[11] They also demonstrated that these reactions occurred slowly at room temperature. Therefore, we examined the stability of the CD·ACA complexes in aqueous solution by UV spectrometric experiment. The molar extinction coefficient values (ε) of ACA and *p*-coumaryl diacetate at 260 nm in ethanol were 250 and 16,830, respectively. The increase rate of the absorbance of free ACA dissolved in 1% ethanol-containing PBS (pH 7.4) at 260 nm was elevated gradually (Fig. 5). This phenomenon indicated the generation of *p*-coumaryl diacetate (or *p*-acetoxycinnamic alcohol) from ACA. Whereas, except for γ-CD·ACA, no significant increase was observed in the case of the CD·ACA complexes (Fig. 5). Thus, it is considered that at least, a rearrangement reaction of ACA in aqueous condition is suppressible by the inclusion into β-CDs. Low stability of γ-CD·ACA complex is probably due to the large cavity for including ACA.

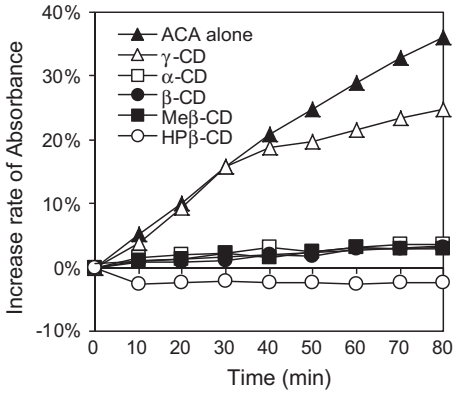

Figure 5. Stability of CD·ACA complexes in aqueous solution. Each sample was dissolved in PBS (pH 7.4) as ACA concentration at 2 mM. The percentages of increase rates of absorbance at 260 nm were plotted as a function of time.

We also evaluated the stability of the CD·ACA complexes in the solid condition. After stored for half a year at 4 °C, ^{1}H NMR spectra of the CD·ACA complexes in D_2O were measured (Fig. 6). Regardless of the solid condition, two acetyl groups of ACA included in both β-CD and Meβ-CD were eliminated and instead new single peak appeared at 2.05 ppm. It is considered that transesterification between two acetoxy groups of ACA and hydroxyl moieties of CDs, or hydrolysis by the existence of H_2O molecules were occurred in the complex. However, no significant chemical shift of ACA was observed in the complexes with HPβ-CD. Therefore, HPβ-CD is the best host molecule for ACA to form a stable, water-soluble complex although the inclusion rate of ACA was somewhat inadequate (63%).

2.4. Apoptotic activity of the CD·ACA complexes

We investigated whether the CD·ACA complexes also induce apoptosis as well as the ACA alone. Evaluation of the cell-death inducing activity of the CD·ACA complexes was carried out by a WST assay. After the HeLa cells were treated with 1–20 μM of the various CD·ACA complexes for 24 h, each cell viability was represented as a percentage of living cells compared to the untreated control cells. As Figure 7A shows, the activity of all CD·ACA complexes were diminished as compared with the ACA alone. Among the CD·ACA complexes, HPβ-CD·ACA maintained high levels of activity at 20 μM, where about 70% of the cells were brought to

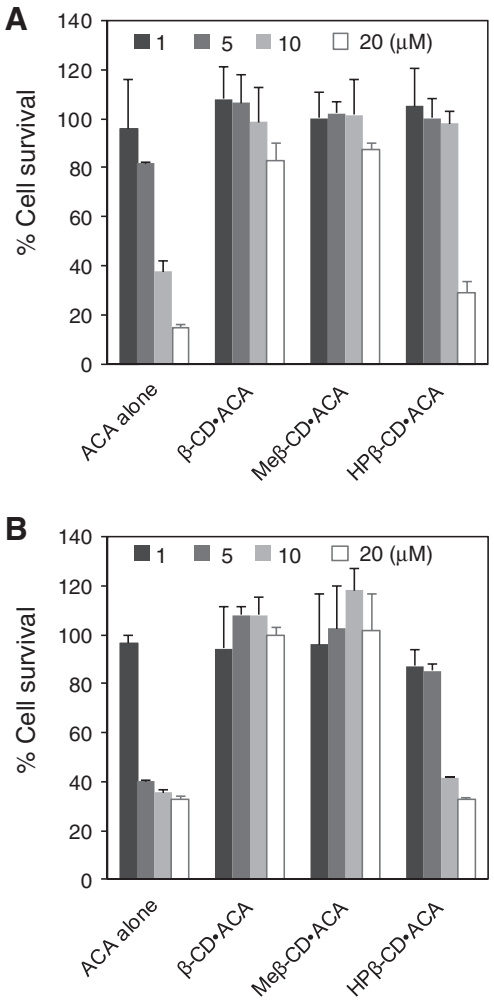

Figure 7. Cytotoxicity of ACA and various CD·ACA complexes against HeLa cells (A) or colon26 cells (B). Cells were treated with the indicated concentrations of each compound for 24 h.

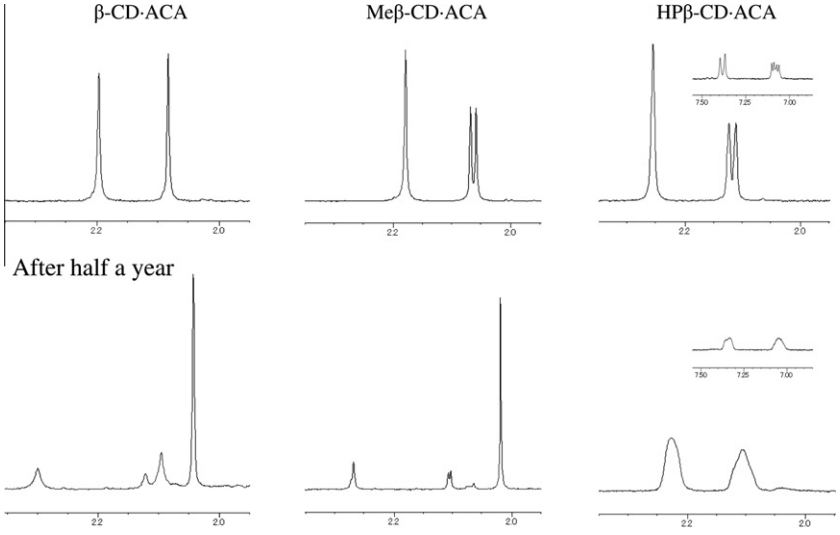

Figure 6. Stability of CD·ACA complexes in the solid condition. After stored for half a year at 4 °C, ^{1}H NMR spectra of the CD·ACA complexes in D_2O were measured. Inset panel showed the peaks corresponding to the aromatic protons of ACA in HPβ-CD·ACA complex.

death. The same study was carried out using murine adenocarcinoma colon26 cells and only HPβ-CD·ACA complex showed cytotoxicity (Fig. 7B).

Caspases, a family of aspartate-specific cysteine proteases, play a crucial role in apoptotic cell death by cleaving a specific site of numerous cellular targets in the execution phase. In particular, caspase-3 was activated by the proteolytic processing of pro-caspase-3 in response to exogenous apoptosis inducers. To determine if HPβ-CD·ACA-induced cell death process for both the HeLa cell and the colon26 cell is apoptosis, we analyzed the level of the activated caspase-3 in the cells treated with HPβ-CD·ACA complex by the Western blot analysis employing a polyclonal anti-active caspase-3 antibody. Figure 8 displays time courses of 6–24 h for the generation of active caspase-3 induced by ACA (20 μM) or HPβ-CD·ACA (20 μM) complex into HeLa or colon26 cells. The activated caspase-3 by the treatment with HPβ-CD·ACA complex was produced at level comparable to that of the ACA alone in both HeLa and colon26 cells. Therefore, HPβ-CD·ACA-induced cell death is due to the activation of the apoptotic process as well as in the case of ACA alone.

2.5. Suppressive effect of the CD·ACA complexes on LPS-stimulated NF-κB activation

Recently, Ichikawa et al. reported that ACA suppressed inflammatory response via the inhibition of the transcription factor NF-κB activation induced by a wide variety of inflammatory agents, including TNF, IL-1β, PMA, LPS and H_2O_2.[19] They also demonstrated that ACA blocked the expression of TNF-induced, antiapoptotic proteins such as survivin, IAP1/2, XIAP, Bcl-2 family members (Bcl-2, BCL-x_L, and Bfl-1/A1) and FLIP, to enhance apoptosis.[19] Most recently, Kleiner-Hancock et al. demonstrated that combination of ACA with all-*trans* retinoic acid, which can suppress Stat3 activation in skin carcinogenesis, significantly inhibited tumor growth of squamous cell carcinoma.[20] Therefore, we investigated whether the CD·ACA complexes also inhibit the NF-κB activation as well as the ACA alone. RAW264.7 cells were pretreated with ACA (5, 10 μM), Meβ-CD·ACA or HPβ-CD·ACA (5, 10 μM) for 30 min and then stimulated with LPS. ACA and HPβ-CD·ACA almost completely inhibited the degradation of IκBα at 5 or 10 μM, respectively (Fig. 9). Meβ-CD·ACA also showed inhibition effect but the activity was weak as compared to that of HPβ-CD·ACA. Degradation of IκBα via phosphorylation allows for translocation of NF-κB from cytosol to nucleus. Therefore, it is considered that HPβ-CD·ACA complex also has suppressive effect on LPS-stimulated NF-κB activation although the activity is slightly weak compared with free ACA.

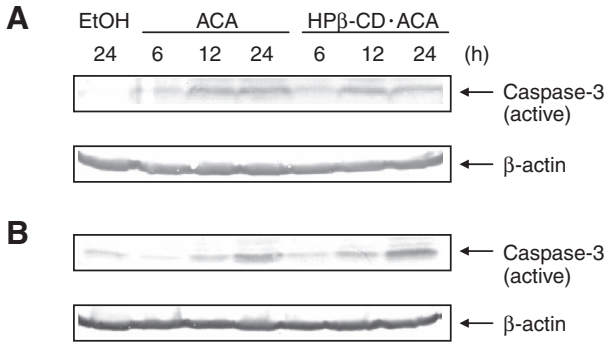

Figure 8. Activation of caspase-3 induced by ACA and HPβ-CD·ACA on HeLa cells (A) or colon26 cells (B). Cells were treated with 20 μM of ACA or HPβ-CD·ACA for various periods (6–24 h). Each cell extract was subjected to Western blot analysis using anti-active caspase-3.

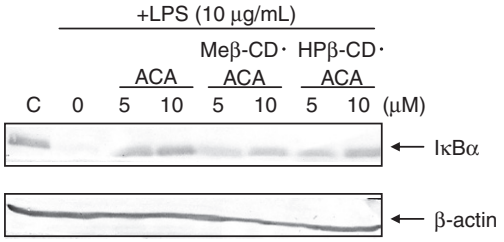

Figure 9. Suppressive effect of the CD·ACA complexes on LPS-stimulated NF-κB activation. RAW264.7 cells were pretreated with ACA (5, 10 μM), Meβ-CD·ACA or HPβ-CD·ACA (5, 10 μM) for 30 min and then stimulated with LPS (10 μg/mL). Each cell extract was subjected to Western blot analysis using anti-IκBα antibody.

2.6. Tumor growth inhibition in mice

Next, we studied the antitumor activity of HPβ-CD·ACA complex in vivo. ACA (5 mg/kg), HPβ-CD·ACA complex (52.5 mg/kg, the molar equivalent to 5 mg/kg of ACA) or vehicle solution was locally injected every other days for 2 weeks. Relative rates of tumor growth were significantly lowered by the administration of both free ACA and HPβ-CD·ACA complex, although the activity of the latter was slightly weak compared with that of the former (Fig. 10A). In fact, tumor weights of mice treatment with free ACA and HPβ-CD·ACA complex for 2 weeks were decreased dominantly as compared with control (Fig. 10B). Consecutive injection of HPβ-CD·ACA complex had no effect on the body weight as well as that of free ACA (Fig. 10C). Thus, both free ACA and HPβ-CD·ACA complex had no toxicity on the mice during the administration. These observations suggest that our water-soluble HPβ-CD·ACA complex maintains the same bioactivity of free ACA.

2.7. Summary

We have succeeded the preparation of the inclusion complexes of β-CDs with ACA by a solid phase HSVM technique. The obtained complexes were water-soluble and had high inclusion rates of ACA (>60%), although the association constants of ACA with CDs in aqueous solution were comparatively small values (<662 M^{-1}). The stability of ACA toward water was also improved by the inclusion in CDs. Among the CD·ACA complexes, only HPβ-CD·ACA complex had the similar characteristics of free ACA although the bioactivity was slightly weak compared with ACA alone. On the other hand, the association constants and the inclusion rates for ACA were similar between HPβ-CD and Meβ-CD. It is likely that the low activity of Meβ-CD·ACA complex is due to its stability in solid condition (Fig. 6). Thus, HPβ-CD·ACA complex may be a better reagent than poorly water-soluble ACA for clinical applications such as anticancer and NF-κB inhibitor drugs.

4. Materials and methods

All materials obtained commercially (guaranteed reagent grade) were used. The racemic ACA was prepared according to our previous method.[21] The obtained compound was a colorless crystal (recrystallized from *n*-hexane, mp 68 °C). α-CD, β-CD, γ-CD, and HPβ-CD were purchased from Sigma Chemical Co. (St. Louis, MO, USA). Meβ-CD and TMβ-CD was purchased from Wako Pure Chemical Industries (Osaka, Japan). ^{1}H NMR and 2D ROESY spectra were determined on Bruker AVANCE300 and Varian UNITY500, respectively. Fluorescence analysis was performed by Hitachi F-7000 fluorescence spectrophotometer. Monoclonal antibody for β-actin was purchased from Abcam (Cambridge, UK). Monoclonal antibody for β-actin was purchased from Abcam (Cambridge, UK). The murine adenocarcinoma colon26 cells (RCB2657) was provided by the

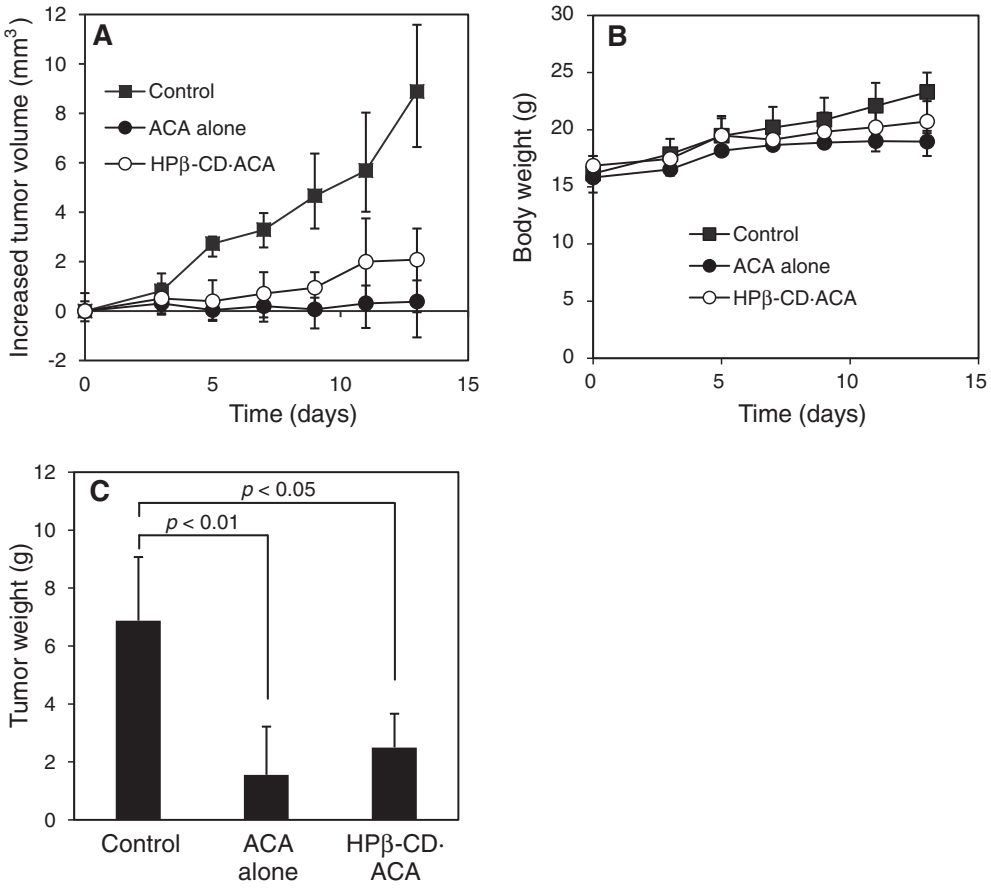

Figure 10. Antitumor effect of HPβ-CD·ACA complex. Control vehicle (PBS containing 1% DMSO, $n = 3$), ACA (5 mg/kg, $n = 3$) or HPβ-CD·ACA (58% inclusion rate, 52.5 mg/kg, $n = 3$) were injected to colon26 cell-bearing BALB/c mice at local injection every other day for 2 weeks. Tumor volume (A) and body weight (B) were measured and calculated every other day as described in Section 4.(C) After 2 weeks of treatment, mice were sacrificed and the tumor weights were determined.

RIKEN BRC through the National Bio-Resource Project of the MEXT, Japan. Female BALB/c mice at 5 weeks of age were obtained from Japan SLC, Inc. (Shizuoka, Japan). The experiments were performed with the permission of the Animal Ethics Committee of Osaka City University in accordance with the Declaration of Helsinki.

4.1. General preparation of the inclusion complexes

β-Cyclodextrin (11.3 mg, 10 μmol)and 5 M equiv of ACA (11.7 mg, 50 μmol) were placed in an agate capsule together with two agate mixing balls and were vigorously mixed by shaking at a rate of 25 Hz for 60 min by the use of a high-speed vibration mill (Retsch, oscillating mill MM200). The solid mixture was dissolved in 10 mL of water and centrifuged at 10,000*g* for 10 min. The resulting supernatant was filtered by a membrane filter (0.22 μm) and lyophilized to obtain the β-CD·ACA complex (12.8 mg). The inclusion rate of the substance ACA was determined by the integrated ratio of seven H1 protons of β-CDs to the aromatic proton *a* (7.3 ppm) of ACA.

4.2. Measurement of the association constants of ACA with various CDs in aqueous solution

The association constants (K) of ACA with various CDs in aqueous solution were estimated by a spectrofluorometric displacement method based on competition between a guest and a fluorescent probe for CDs described by Tee et al.[15] Briefly, association constants (K_{ANS}) of sodium 1-anilino-8-naphthalenesulfonate (ANS) with β-CD, Meβ-CD, and HPβ-CD were firstly measured in PBS solution (pH 7.4). A stock solution of ANS (10 mM in PBS) was added to each PBS solution containing β-CD (0–12 mM), Meβ-CD and HPβ-CD (0–1.2 mM), and each mixture was stored for 2 h at 25 °C in dark. The final concentration of ANS was 10 μM. Each sample was irradiated at 365 nm and the fluorescence intensity (I_{obs}) was measured at 500 nm for β-CD, 480 nm for Meβ-CD and HPβ-CD. The obtained values were converted into relative fluorescence intensity, using $F_{rel} = I_{obs}/I_0$ (I_0: the intensity of CD-free solution). In the case of the formation of 1:1 complex between CD and ANS, the relative fluorescence F_{rel} varies with the concentration of CD in accord with Eq. 1. On the basis of Eq. 1, a typical plot is shown in Fig. 1A. Values of K_{ANS} and F_c were estimated from nonlinear fitting of Eq. 1 and listed in Table 1.

From the initial CD and ANS concentrations ($[CD]_0$ and $[ANS]_0$, respectively), the actual $[ANS]$ was calculated by solving the Eq. 2:

$$[ANS]^2 + (1/K_{ANS} + [CD]_0 - [ANS]_0)[ANS] - [ANS]_0/K_{ANS} = 0 \quad (2)$$

Next, free CD concentration ($[CD]$) was obtained by Eq. 3 and the reference fluorescence (F_{ref}), which is a relative fluorescence intensity in the absent of ACA, was evaluated from Eq. 1.

$$[CD] = [CD]_0 - [ANS]_0 + [ANS] \quad (3)$$

The fluorescence intensities (I_{obs}) in the presence of ACA were converted to the F_{rel} values using the Eq. 4 (I_{ng}: fluorescence intensity with no guest present):

$$F_{rel} = \frac{I_{obs}F_{ref}}{I_{ng}} \quad (4)$$

The actual free CD concentrations ([*CD*]) in the presence of various $[ACA]_0$ were calculated by the Eq. 5 and the association constant values (K) of CD with ACA were obtained by the Eq. 6:

$$[CD] = \frac{(F_{rel} - 1)}{K_{ANS}(F_c - F_{rel})} \quad (5)$$

$$K = \frac{([CD]_0 - [CD])}{[CD]([ACA]_0 - [CD]_0 + [CD])} \quad (6)$$

The average Ks of the individual values for various CDs were listed in Table 1.

4.3. Stability of ACA and CD·ACA complexes by UV spectrometric analysis

CD·ACA complexes were dissolved in PBS (pH 7.4) at 2 mM of ACA concentration and the absorbance of each sample solution at 260 nm was measured on a NanoDrop ND-1000 spectrophotometer. For free ACA, the stock solution (200 mM, in ethanol) was diluted into PBS at a final concentration of 2 mM, and measured immediately. The percentages of increase rates of absorbance were plotted as a function of time (Fig. 5).

4.4. Cell culture

HeLa cells (human epithelial carcinoma), colon26 cells (murine adenocarcinoma) and RAW264.7 cells (murine monocyte/macrophage) were grown in Dulbecco's modified eagle media (DMEM) containing 10% heat-incubated fetal bovine serum (FBS) supplemented with streptomycin and penicillin at 37 °C with 5% CO_2 atmosphere. ACA was dissolved in ethanol at 1–20 mM, and added to the cells as ethanol solutions. CD·ACA complexes were dissolved in PBS at 10–200 mM of ACA concentration. The final concentrations of both ethanol and PBS were 0.1% and 1%, respectively. Control experiments were performed with ethanol (0.1%) and PBS (1%) as the vehicle for WST assay and no cytotoxic effect were observed in both two vehicles-treated cells (data not shown).

4.5. WST assay

HeLa or colon26 cells were seeded at a density of 10^4 cells/well in a 96-well microtiter plate. Following 24 h of incubation the medium was removed and washed in PBS, then replaced with fresh media containing the CD·ACA complexes or ACA alone (1–20 μM). The cells were further incubated for 22 h and then treated with a Cell Counting Kit-8® (Dojindo, Kumamoto, Japan) for 2 h. Cell viability was estimated from the absorbance of medium at 620 and 450 nm by using a Multiscan Ascent microplate reader (Thermo Labsystems). The percent of cell viability in the absence of a polyelectrolyte was normalized to 100%. All data were the average of at least three separate determinations.

4.6. Immunoblot analysis for the detection of active caspase-3

HeLa and colon26 cells were seeded at a density of 0.5×10^6 cells/well in 1 mL of the growth medium in 6-well plates. Following 24 h of incubation the medium was removed and washed in PBS, then replaced with fresh DMEM containing CD·ACA (20 μM) for various periods. After incubation for various periods, cells were collected and centrifuged at 400 *g* for 5 min at 4 °C, washed twice with PBS and lysed in 50 μL of lysis buffer [62.5 mM Tris–HCl (pH 6.8), 6 M urea, 10% glycerol, 2% SDS, 0.00125% bromophenol blue, 5% β-mercaptoethanol]. Cell lysates were boiled for 3 min and separated on 14% SDS–polyacrylamide gel, transferred to a polyvinylidene difluoride membrane, and probed with rabbit polyclonal anti-active caspase-3 antibody or monoclonal anti-β-actin antibody, followed by probing with goat anti-rabbit antibody (for caspase-3) or anti-mouse antibody (for β-actin) coupled to alkaline phosphatase.

4.7. Immunoblot analysis for the detection of IκBα

Raw264.7 cells were seeded at a density of 0.5×10^6 cells/well in 1 mL of the growth medium in 6-well plates. Following 24 h of incubation ACA or CD·ACA were added at a final concentration of 5 and 10 μM. After pre-incubation for 30 min, LPS was added at a final concentration of 10 μg/mL. After incubation for 15 min, cells were removed using a cell scraper and collected into 1.5 mL eppendorf tubes. After centrifugation at 400*g* for 5 min at 4 °C, cells were washed twice with PBS and lysed in 50 μL of lysis buffer. Cell lysates were boiled for 3 min and separated on 12% SDS–polyacrylamide gel, transferred to a polyvinylidene difluoride membrane, and probed with rabbit polyclonal anti-IκBα antibody or monoclonal anti-β-actin antibody, followed by probing with goat anti-rabbit antibody (for IκBα) or anti-mouse antibody (for β-actin) coupled to alkaline phosphatase.

4.8. Tumor growth inhibition of the HPβ-CD·ACA complex in mice

Colon26 cells were pre-cultured in DMEM containing 10% FBS supplemented with streptomycin and penicillin and 6×10^5 cells were intradermally inoculated into BALB/c mice. Two weeks after the implantation of the cells, the tumor-bearing mice were randomly divided into three groups ($n = 3$) and locally injected with PBS (containing 1% DMSO), 5 mg/kg ACA (dissolved with PBS containing 1% DMSO) or 52.5 mg/kg HPβ-CD·ACA (58% inclusion rate, dissolved with PBS) every other days for 2 weeks. The size of the tumor was calculated by; volume (mm^3) = 0.5 × major axis (mm) × (minor axis (mm))^2. After 2 weeks of treatment, the mice were sacrificed and dissected to measure the tumor weights.

References and notes

1. Moffatt, J.; Hashimoto, M.; Kojima, A.; Kennedy, D. O.; Murakami, A.; Koshimizu, K.; Ohigashi, H.; Matsui-Yuasa, I. *Carcinogenesis* **2000**, *21*, 2151.
2. Ohnishi, H.; Asamoto, M.; Tujimura, K.; Hokaiwado, N.; Takahashi, S.; Ogawa, K.; Kuribayashi, M.; Ogiso, T.; Okuyama, H.; Shirai, T. *Cancer Sci.* **2004**, *95*, 936.
3. Zheng, Q.; Hirose, Y.; Yoshimi, N.; Murakami, A.; Koshimizu, K.; Ohigashi, H.; Sakata, K.; Matsumoto, Y.; Sayama, Y.; Mori, H. J. *Cancer Res. Clin. Oncol.* **2002**, *128*, 539.
4. Awang, K.; Azmi, M. N.; Aun, L. I.; Aziz, A. N.; Ibrahim, H.; Nagoor, N. H. *Molecules* **2010**, *15*, 8048.
5. Matsuda, H.; Morikawa, T.; Managi, H.; Yoshikawa, M. *Bioorg. Med. Chem. Lett.* **2003**, *13*, 3197.
6. Ye, Y.; Li, B. *J. Gen. Virol.* **2006**, *87*, 2047.
7. Matsuda, H.; Ando, S.; Morikawa, T.; Kataoka, S.; Yoshikawa, M. *Bioorg. Med. Chem. Lett.* **2005**, *15*, 1949.
8. Morikawa, T.; Ando, S.; Matsuda, H.; Kataoka, S.; Muraoka, O.; Yoshikawa, M. *Chem. Pharm. Bull (Tokyo)* **2005**, *53*, 625.
9. Ando, S.; Matsuda, H.; Morikawa, T.; Yoshikawa, M. *Bioorg. Med. Chem.* **2005**, *13*, 3289.
10. Xu, S.; Kojima-Yuasa, A.; Azuma, H.; Kennedy, D. O.; Konishi, Y.; Matsui-Yuasa, I. *Chem. Biol. Interact.* **2010**, *185*, 235.
11. Yang, X.; Eilerman, R. G. *J. Agric. Food Chem.* **1999**, *47*, 1657.
12. Ishizu, T.; Kajitani, S.; Tsutsumi, H.; Yamamoto, H.; Harano, K. *Magn. Reson. Chem.* **2008**, *46*, 448.
13. Lucas-Abellán, C.; Gabaldón-Hernández, J. A.; Penalva, J.; Fortea, M. I.; Núñez-Delicado, E. *J. Agric. Food Chem.* **2008**, *56*, 8081.
14. Komatsu, K.; Fujiwara, K.; Murata, Y.; Braun, T. *J. Chem. Soc., Perkin Trans. 1* **1999**, 2963.
15. Ikeda, A.; Hayashi, K.; Konishi, T.; Kikuchi, J. *Chem. Commun.* **2004**, 1334.
16. Tee, O. S.; Gadosy, T. A.; Giorgi, J. B. *Can. J. Chem.* **1996**, *74*, 736.
17. Selvidge, L. A.; Eftink, M. R. *Anal. Biochem.* **1986**, *154*, 400.

18. Raffaini, G.; Ganazzoli, F.; Malpezzi, L.; Fuganti, C.; Fronza, G.; Panzeri, W.; Mele, A. *J. Phys. Chem. B* **2009**, *113*, 9110.
19. Ichikawa, H.; Takada, Y.; Murakami, A.; Aggarwal, B. B. *J. Immunol.* **2005**, *174*, 7383.
20. Kleiner-Hancock, H. E.; Shi, R.; Remeika, A.; Robbins, D.; Prince, M.; Gill, J. N.; Syed, Z.; Adegboyega, P.; Mathis, J. M.; Clifford, J. L. *BMC Cancer* **2010**, *10*, 394.
21. Azuma, H.; Miyasaka, K.; Yokotani, T.; Tachibana, T.; Kojima-Yuasa, A.; Matsui-Yuasa, I.; Ogino, K. *Bioorg. Med. Chem.* **2006**, *14*, 1811.